

Supporting Information for

Effects of Submarine Groundwater on Nutrient Concentration and Primary Production in a Deep Bay of the Japan Sea

Menghong Dong¹, Xinyu Guo^{2*}, Takuya Matsuura³, Taichi Tebakari⁴, and Jing Zhang⁵

¹State Key Laboratory of Satellite Ocean Environment Dynamics, Second Institute of Oceanography, Ministry of Natural Resources, Hangzhou, China

²Center for Marine Environmental Studies, Ehime University, Matsuyama, Japan

³Graduate Faculty of Interdisciplinary Research Faculty of Engineering, Civil Engineering and Environmental Engineering, Yamanashi University, Koufu, Japan

⁴Civil, Human and Environmental Science and Engineering Course, Graduate School of Science and Engineering, Chuo University, Tokyo, Japan

⁵Faculty of Science, Academic Assembly, University of Toyama, Toyama, Japan

*Corresponding author: Xinyu Guo (guo.xinyu.mz@ehime-u.ac.jp), Orcid ID: 0000-0002-4832-8625

Contents of this file

Text S1 to S5

Table S1

Figures S1 to S13

Introduction

This supporting information contains additional descriptions of the model configuration and results (Text S1 to S5), one table (S1) and 13 figures (S1-S13).

Text S1.

A three-dimensional, free surface, primitive equation ocean model was used. It includes thermodynamics and the level 2.5 Mellor-Yamada turbulence closure and uses a sigma coordinate in the vertical to resolve the variation of bottom topography (Blumberg & Mellor, 1987; Mellor, 1998). This model assumes the hydrostatic balance and can be used to solve the nonlinear primitive external and internal mode equations on the Arakawa C-grid system.

Text S2.

Onitsuka and Yanagi (2005) applied two ecosystem models differing in ecological complexity: the NPZD and a nine-compartment model that includes two categories of phytoplankton and three categories of zooplankton, to the northern and southern parts of the Japan Sea with the same biochemical parameters and compared the results of the two models. Their results indicated that the seasonal variations in several variables (such as Chlorophyll-a, nitrate, and primary production) are not significantly different between the two models, and with a careful selection of biochemical parameter values, the NPZD model could calculate the seasonal variations of those variables in the Japan Sea.

Text S3.

The biogeochemical processes in this study are based on nitrogen (Figure S2). The processes related to phosphate were calculated based on a Redfield ratio of 16:1 (N: P). The biogeochemical processes are described as follows:

$$\begin{aligned} Bio(DIN) = & \text{Respiration} + \text{Excretion} \\ & + \text{Decomposition} - \text{Photosynthesis}, \end{aligned} \quad (S1)$$

$$\begin{aligned} Bio(PHY) = & \text{Photosynthesis} - \text{Respiration} \\ & - \text{Mortality}(PHY) - \text{Grazing} - \text{Sinking}, \end{aligned} \quad (S2)$$

$$\begin{aligned} Bio(ZOO) = & \text{Grazing} - \text{Mortality}(ZOO) \\ & - \text{Egestion} - \text{Excretion}, \end{aligned} \quad (S3)$$

$$\begin{aligned} Bio(DET) = & \text{Mortality}(PHY) + \text{Mortality}(ZOO) \\ & + \text{Egestion} - \text{Decomposition} - \text{Sinking}, \end{aligned} \quad (S4)$$

$$\begin{aligned} Bio(DIP) = & (\text{Respiration} + \text{Excretion} \\ & + \text{Decomposition} - \text{Photosynthesis})/16, \end{aligned} \quad (S5)$$

Each term of the compartment can be expressed in the forms given below. Photosynthesis is doubled as the water temperature increases by 10 °C (Eppley, 1972). An almost identical assumption was adopted for other processes that depend on temperature. The parameter values are shown in Table S1.

$$\begin{aligned} \text{Photosynthesis} = & V_{max} \times \min \left\{ \frac{DIN}{DIN + K_{DIN}}, \frac{DIP}{DIP + K_{DIP}} \right\} \\ & \times \exp(k_{pho}T) \times \frac{I}{I_{opt}} \exp\left(1 - \frac{I}{I_{opt}}\right) \times PHY, \end{aligned} \quad (S6)$$

$$I = I_0 \exp\left(-\int_0^z k_e dz\right), \quad (S7)$$

$$k_e = \alpha_1 + \alpha_2 \times PHY, \quad (S8)$$

$$\text{Respiration} = P_{res} \times \exp(k_{res}T) \times PHY, \quad (S9)$$

$$Mortality(PHY) = P_{mor} \times \exp(k_{mor1}T) \times PHY^2, \quad (S10)$$

$$Grazing = G_{max} \times \max\{0, 1 - \exp[\lambda(\sigma - PHY)]\} \\ \times \exp(k_{gra}T) \times ZOO, \quad (S11)$$

$$Excretion = (\alpha_z - \beta_z) \times Grazing, \quad (S12)$$

$$Egestion = (1 - \alpha_z) \times Grazing, \quad (S13)$$

$$Mortality(ZOO) = Z_{mor} \times \exp(k_{mor2}T) \times ZOO^2, \quad (S14)$$

$$Decomposition = D_{dec} \times \exp(k_{dec}T) \times DET, \quad (S15)$$

$$Sinking_{PHY} = \frac{\partial}{\partial z} (S_{PHY} \times PHY), \quad (S16)$$

$$Sinking_{DET} = \frac{\partial}{\partial z} (S_{DET} \times DET), \quad (S17)$$

where I is the light intensity, k_e is the dissipation coefficient, I_0 is the photosynthetically active radiation at the surface, which is considered to be 40% of the shortwave radiation at the surface, and T is the water temperature. A portion (40%) of the surface shortwave radiation data from the GPV-MSM, namely the photosynthetically active radiation, was used as the surface light intensity in photosynthesis (Sarmiento & Gruber, 2006).

Text S4.

Each biogeochemical process supported by different source nutrients in the tracking module can be expressed as follows:

$$Bio_x(DIN) = Respiration \times \frac{PHY_x}{PHY} + Excretion \times \frac{ZOO_x}{ZOO} \\ + Decomposition \times \frac{DET_x}{DET} - Photosynthesis \times \frac{DIN_x}{DIN}, \quad (S18)$$

$$Bio_x(PHY) = Photosynthesis \times \frac{DIN_x}{DIN} - Respiration \times \frac{PHY_x}{PHY} \\ - Mortality(PHY) \times \frac{PHY_x}{PHY} - Grazing \times \frac{PHY_x}{PHY} - Sinking, \quad (S19)$$

$$Bio_x(ZOO) = Grazing \times \frac{PHY_x}{PHY} - Mortality(ZOO) \times \frac{ZOO_x}{ZOO} \\ - Egestion \times \frac{ZOO_x}{ZOO} - Excretion \times \frac{ZOO_x}{ZOO}, \quad (S20)$$

$$Bio_x(DET) = Mortality(PHY) \times \frac{PHY_x}{PHY} + Mortality(ZOO) \\ \times \frac{ZOO_x}{ZOO} + Egestion \times \frac{ZOO_x}{ZOO} - Decompositon \times \frac{DET_x}{DET} - Sinking, \quad (S21)$$

where X can be any of three external sources of nutrient or residual nutrient, i.e., JS, RV, GW, and RE.

Text S5.

The vertical distribution of nutrients in the center of the bay is similar to that in the Japan Sea. High-concentration nutrients are distributed along the coastal area of the bay throughout the year. Phytoplankton are distributed mainly in the upper 100 m and have a remarkable spring bloom when a high concentration of phytoplankton is found up to a depth of 50 m below the surface. Since May, the phytoplankton has decreased throughout the bay except for the estuary area where nutrients are supplied from the rivers. In addition, from May to September, the subsurface chlorophyll maximum appears at approximately 30 m. The changes in zooplankton and detritus coincide with the changes in phytoplankton.

Table S1. Model validation. rmsd: root mean square deviation; r^2 : the coefficient of determination.

	Temperature		Salinity		DIN		Phytoplankton	
	rmsd (°C)	r^2	rmsd (psu)	r^2	rmsd (mmolN m ⁻³)	r^2	rmsd (mmolN m ⁻³)	r^2
Jan	1.04	0.92	0.15	0.76	2.01	0.90	0.07	0.61
Feb	1.26	0.81	0.12	0.50	2.14	0.93	0.08	0.59
Mar	1.14	0.78	0.16	0.63	0.05	0.96	—	—
Apr	0.90	0.86	0.16	0.85	1.82	0.96	0.06	0.91
May	1.22	0.86	0.27	0.53	1.79	0.95	0.09	0.73
Jun	1.40	0.89	0.23	0.67	1.78	0.96	0.08	0.78
Jul	1.73	0.92	0.25	0.63	2.76	0.90	0.09	0.58
Aug	1.71	0.95	0.26	0.68	2.20	0.93	0.11	0.62
Sep	1.75	0.95	0.30	0.71	—	—	0.06	0.83
Oct	1.34	0.96	0.28	0.75	1.65	0.96	0.09	0.59
Nov	1.16	0.96	0.22	0.75	1.30	0.98	0.06	0.79
Dec	1.06	0.95	0.20	0.66	1.42	0.97	0.02	0.94
Mean	1.75	0.92	0.26	0.64	2.25	0.93	0.08	0.65

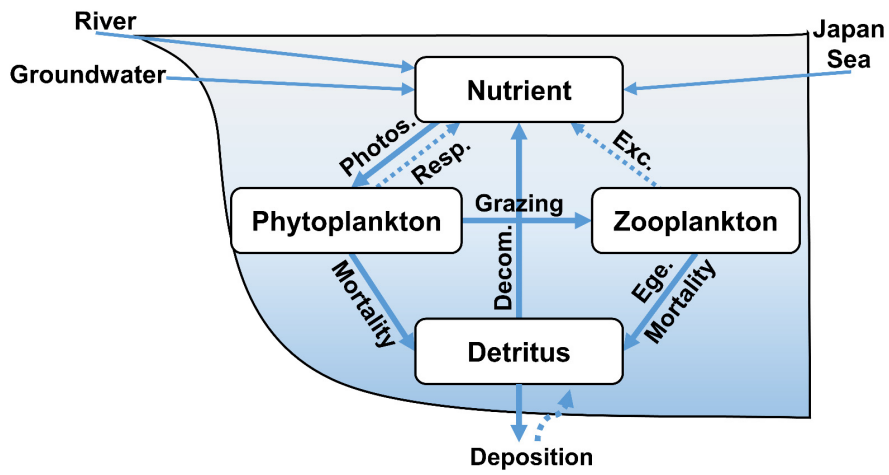
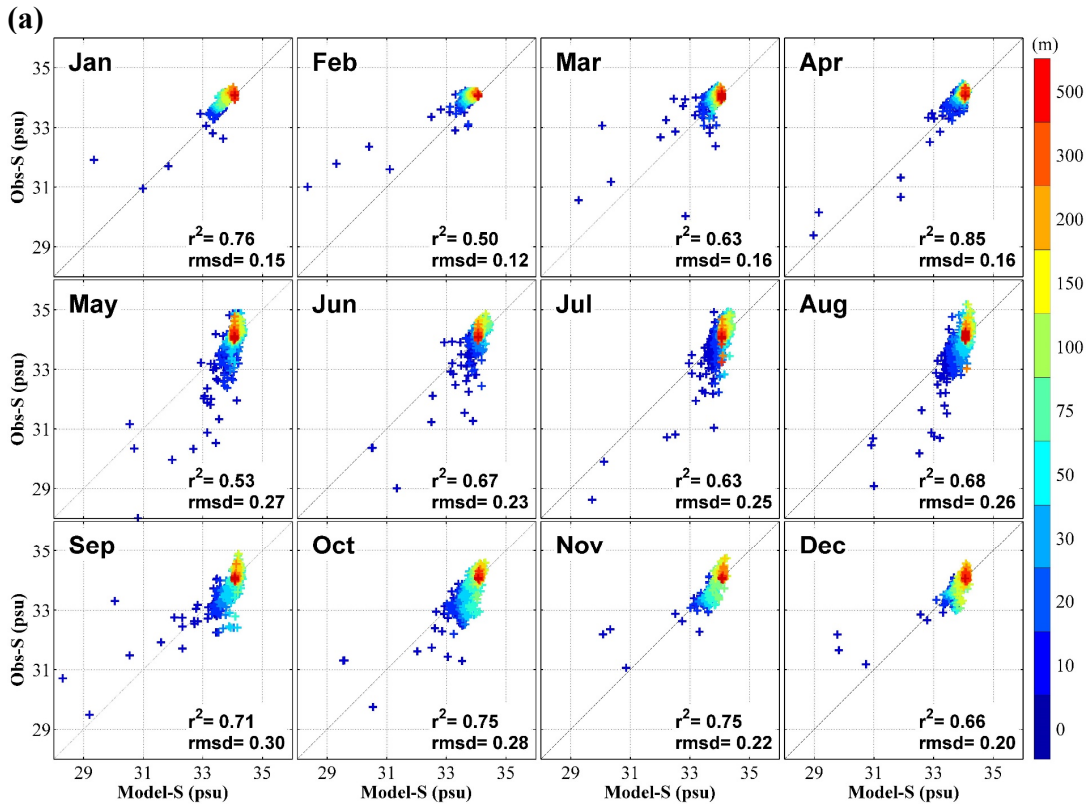
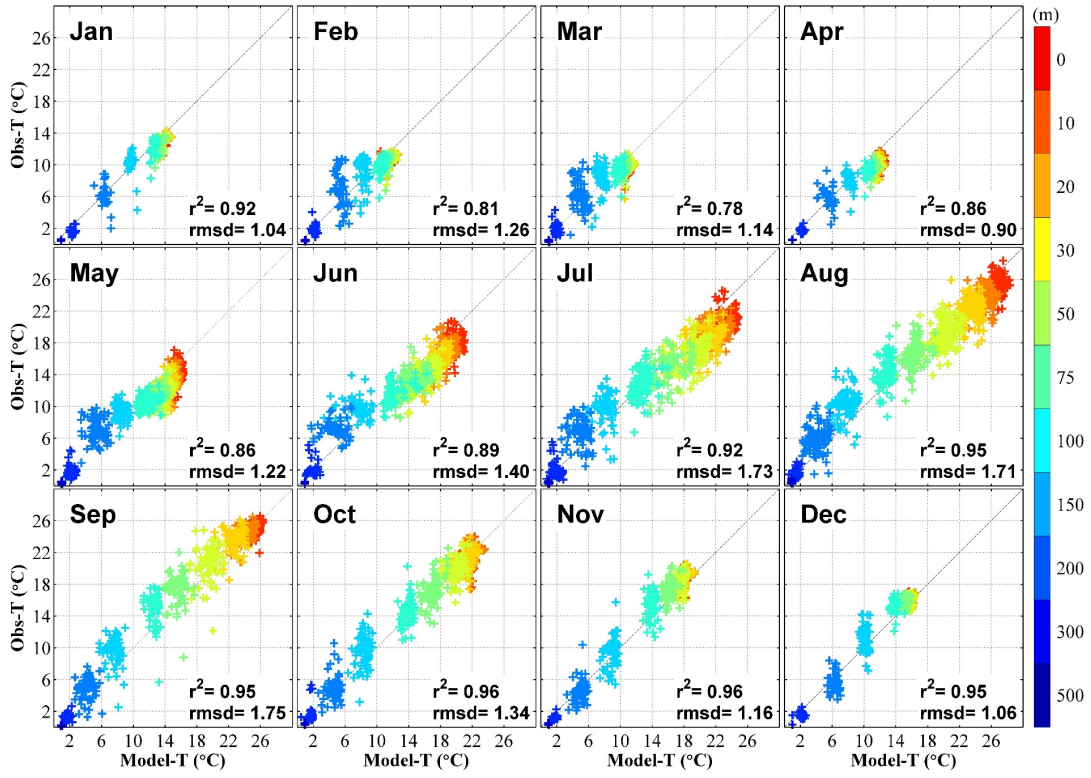
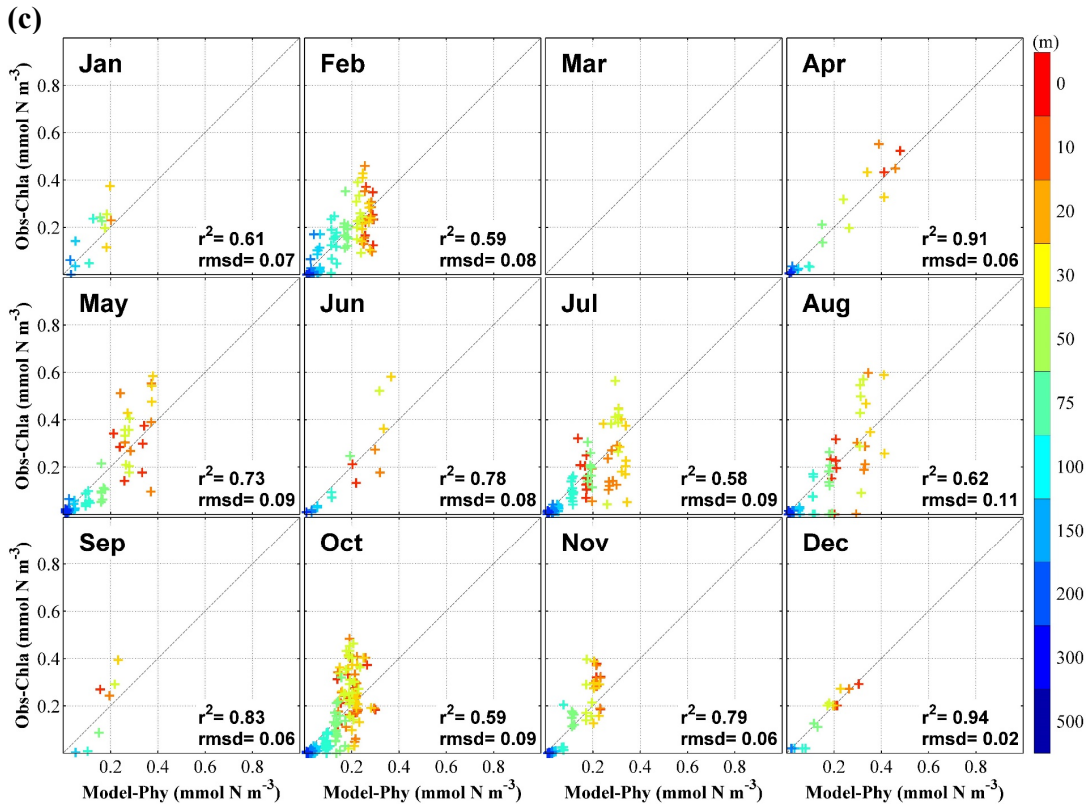
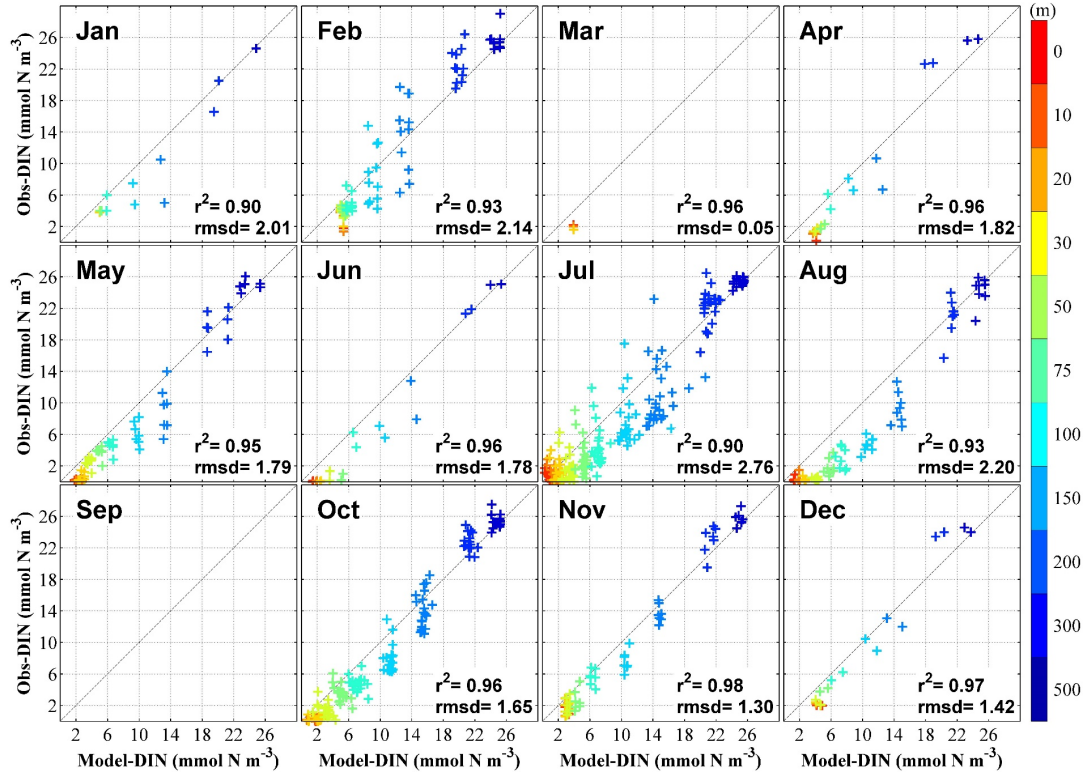


Figure S1. Biogeochemical processes in the ecosystem model. In this model, groundwater is released at the bottom of the sea. Photos., Resp., Exc., Ege., and Decom. represent Photosynthesis, Respiration, Excretion, Egestion, and Decomposition, respectively.



(b)



(d)

Figure S2. Scatter plot of monthly data and model results for (a) Water temperature, (b) Salinity, (c) Dissolved inorganic nitrogen (DIN), and (d) Chl.a. The colors represent water depths.

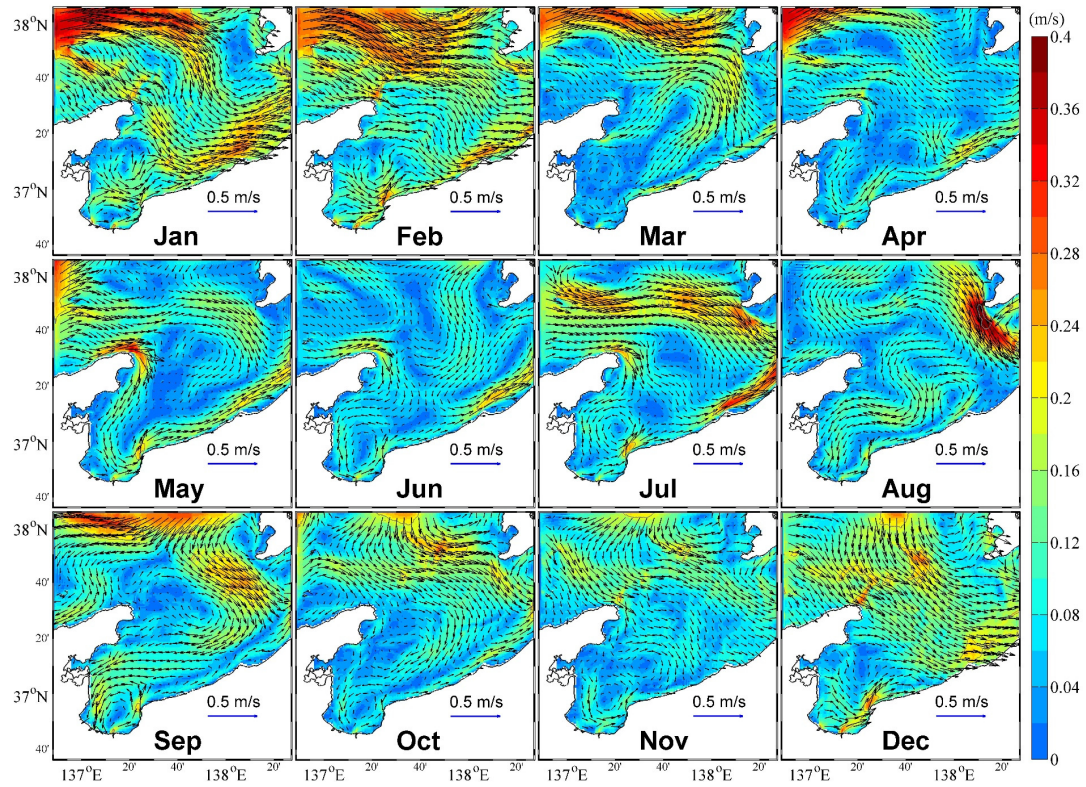


Figure S3. Mean monthly surface current. The black arrows represent the current direction and the colors represent the magnitude of the current.

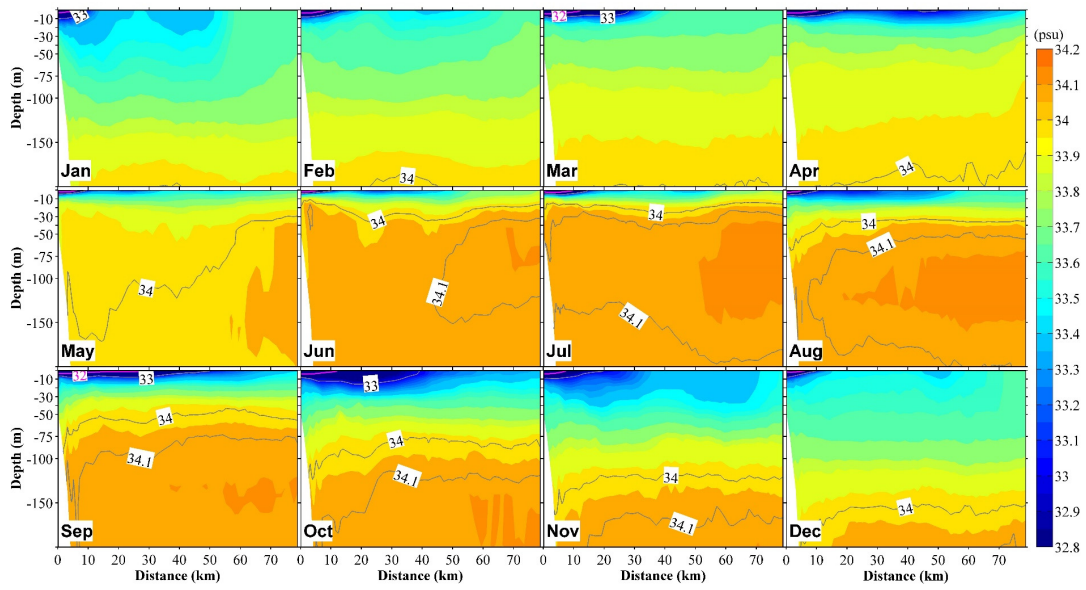


Figure S4. Vertical section (S2 in Figure 1b) of the distributions of salinity in different months.

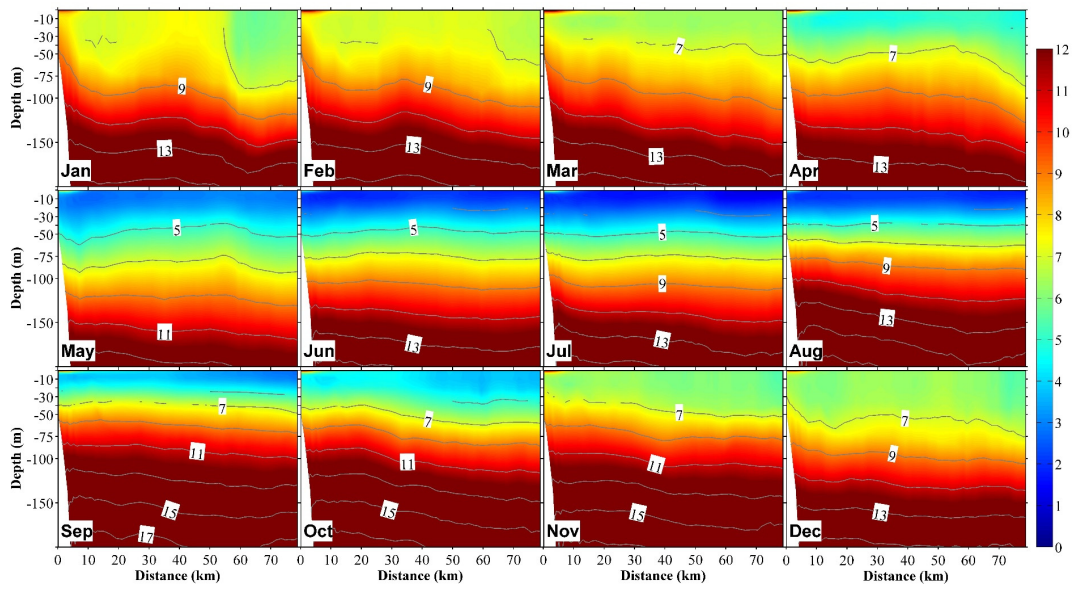
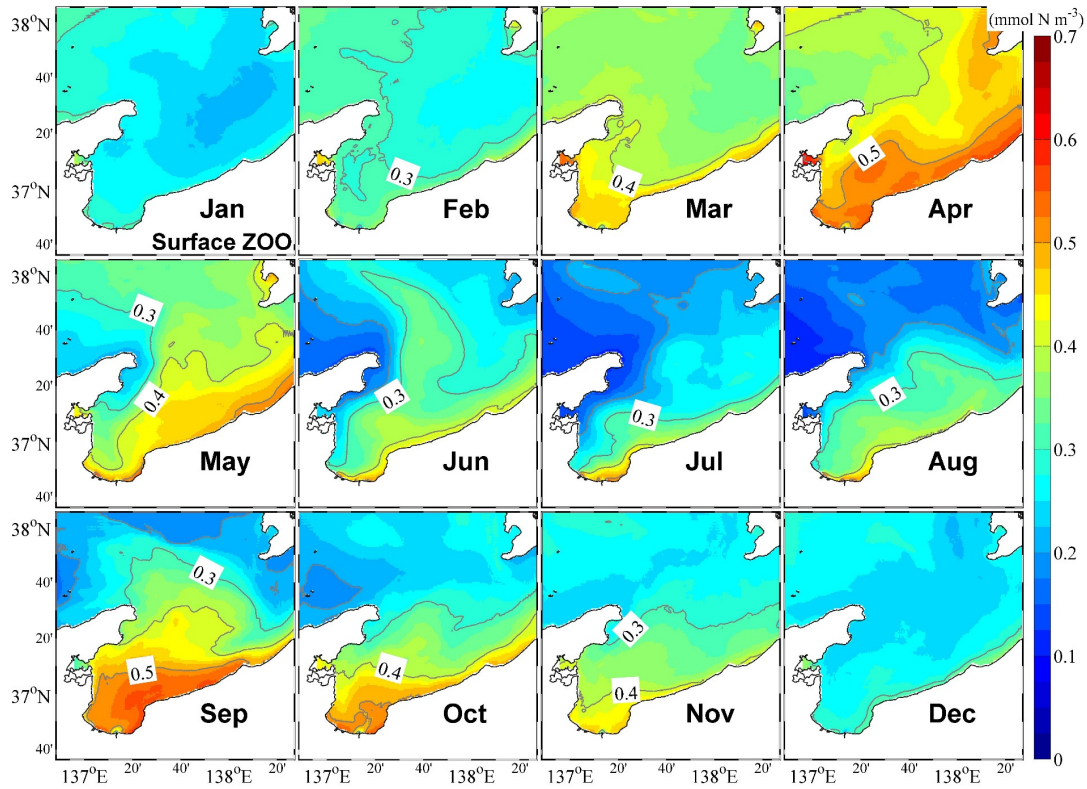
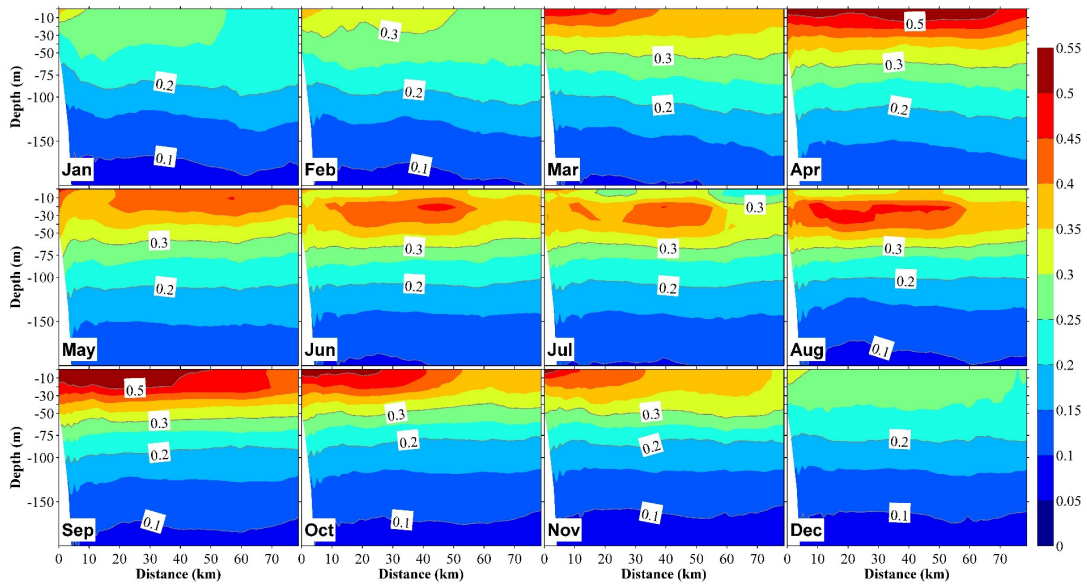


Figure S5. Vertical section (S2 in Figure 1b) of the distributions of dissolved inorganic nitrogen (DIN) in different months.

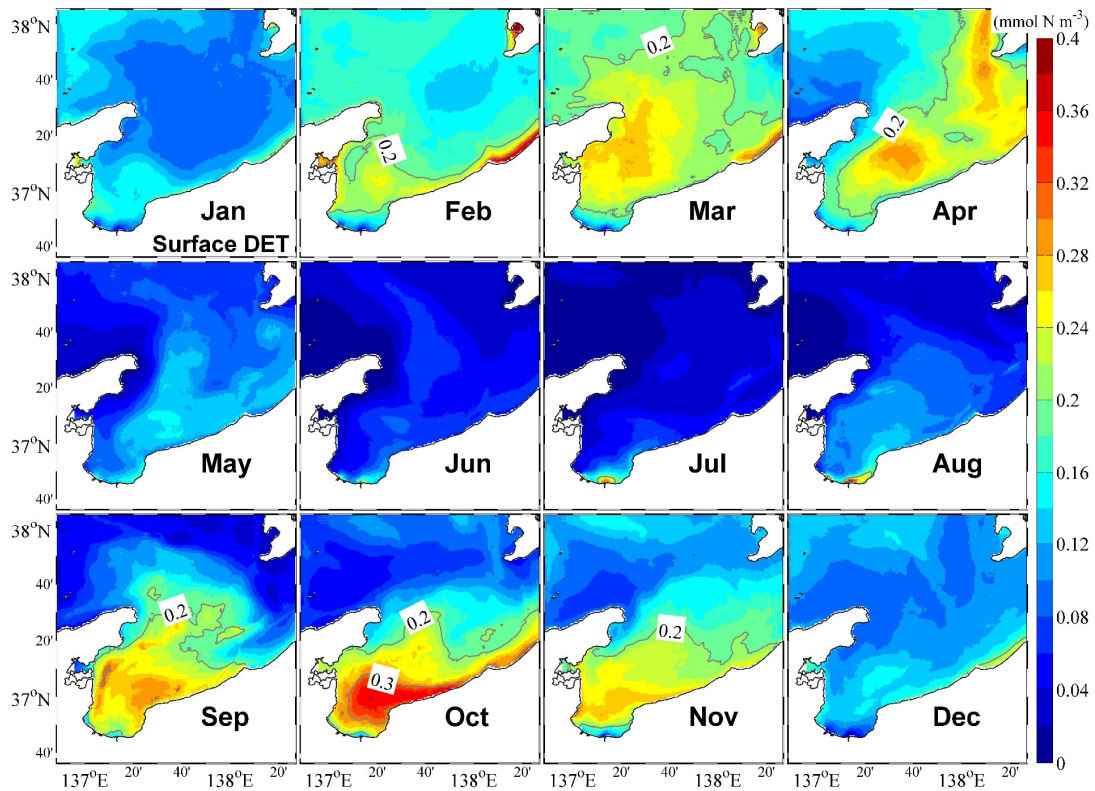


(a)

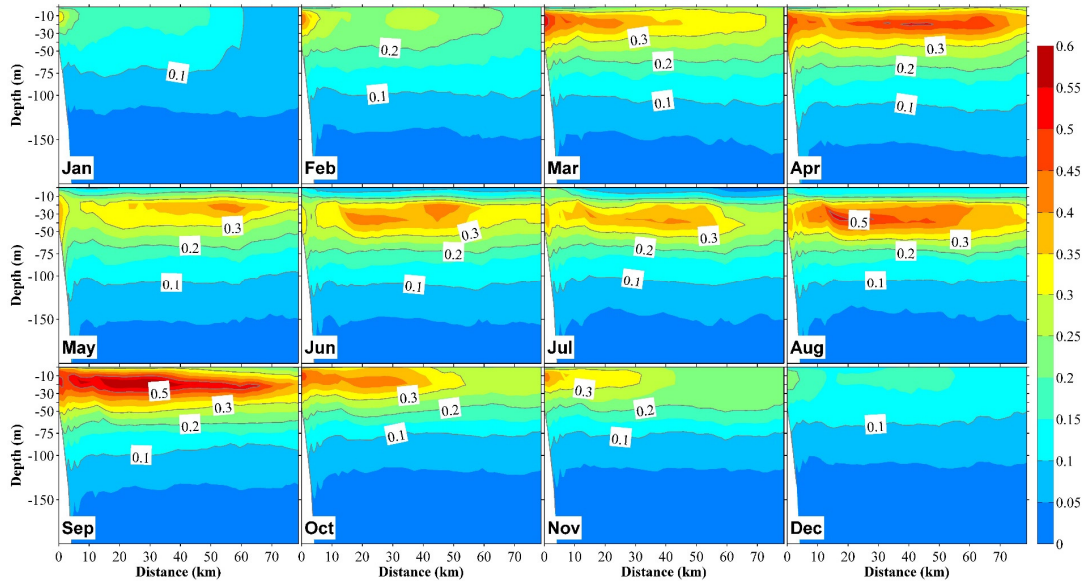


(b)

Figure S6. Distribution of zooplankton concentrations. (a) Mean monthly mean surface zooplankton. (b) Vertical section (S2 in Figure 1b) of the distribution of zooplankton.



(a)



(b)

Figure S7. Distribution of detritus (DET). (a) Mean monthly mean surface DET, (b) Vertical section (S2 in Figure 1b) of the distribution of DET.

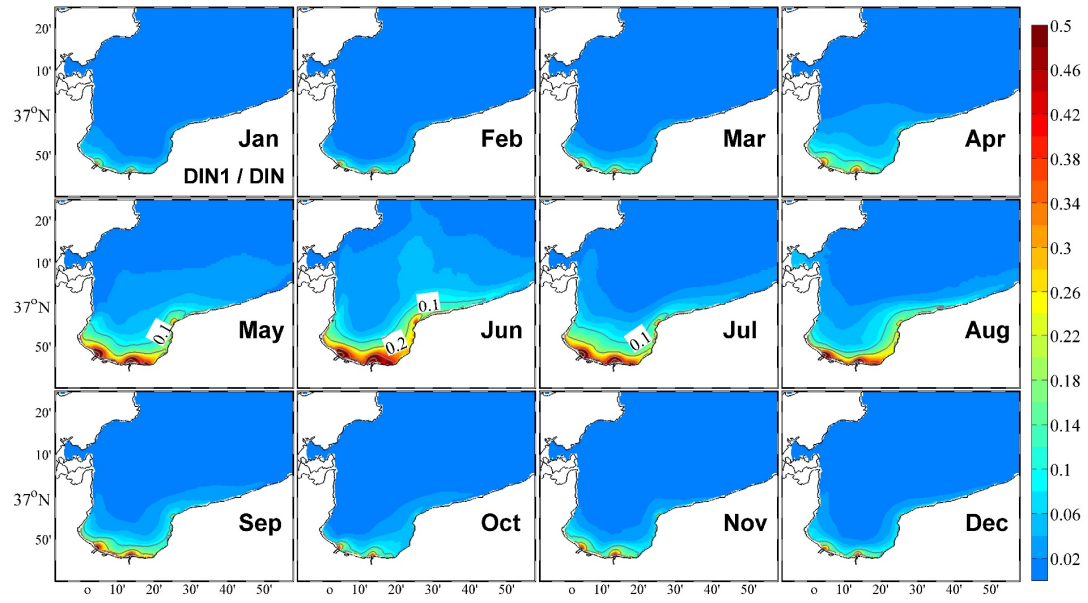


Figure S8. Contributions of dissolved inorganic nitrogen (DIN) originating from river water to total DIN in the surface layer (0–20 m).

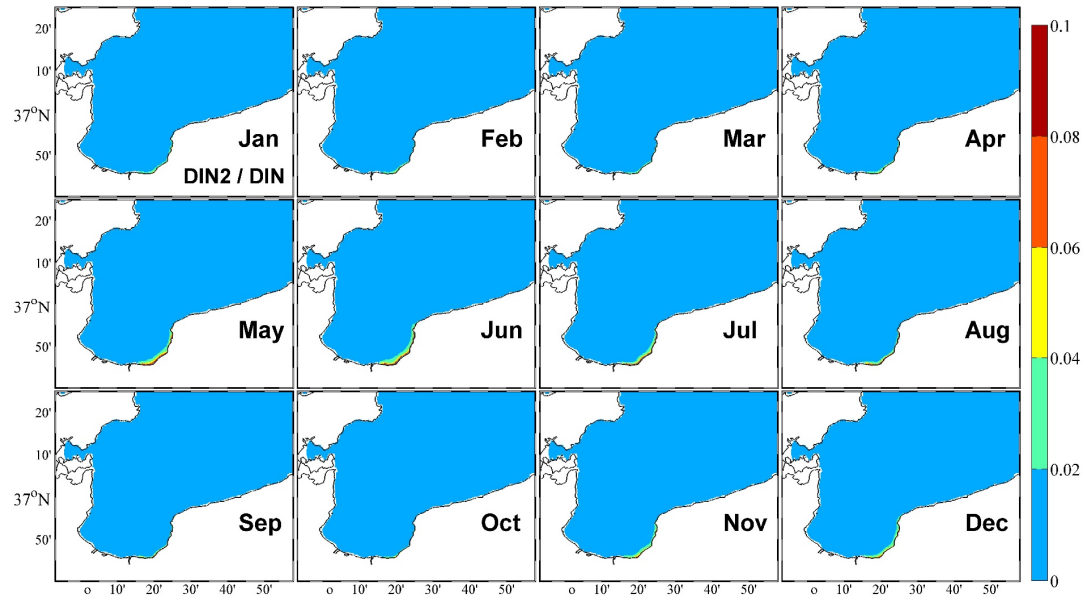


Figure S9. Contributions of dissolved inorganic nitrogen (DIN) originating from submarine groundwater discharge (SGD) to the total DIN in the upper layer (0–70 m) in different months.

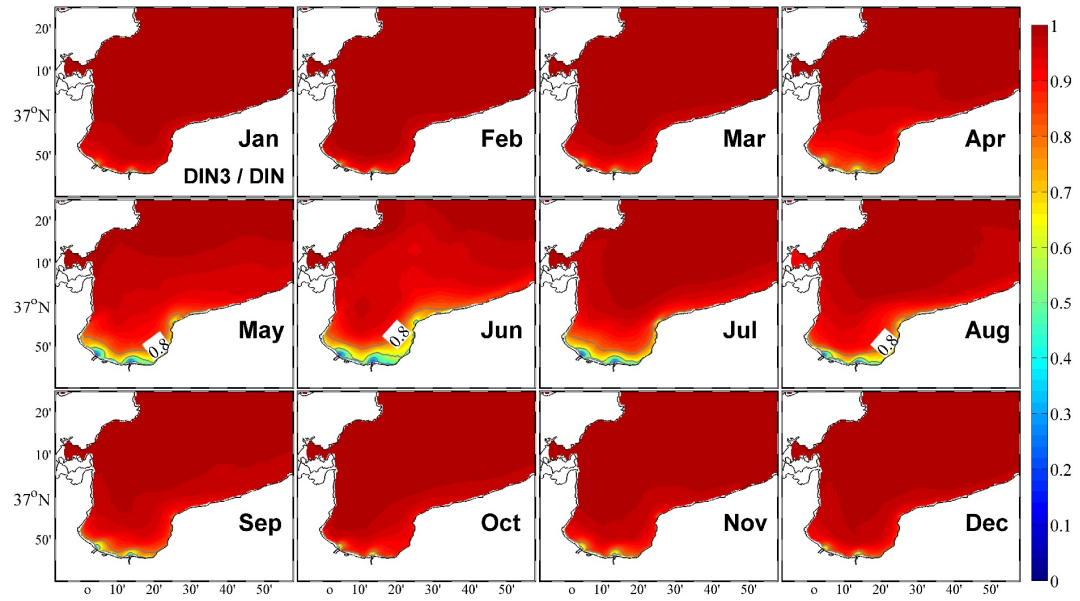


Figure S10. Contributions of dissolved inorganic nitrogen (DIN) originating from the Japan Sea to total DIN in the surface layer (0–20 m) in different months.

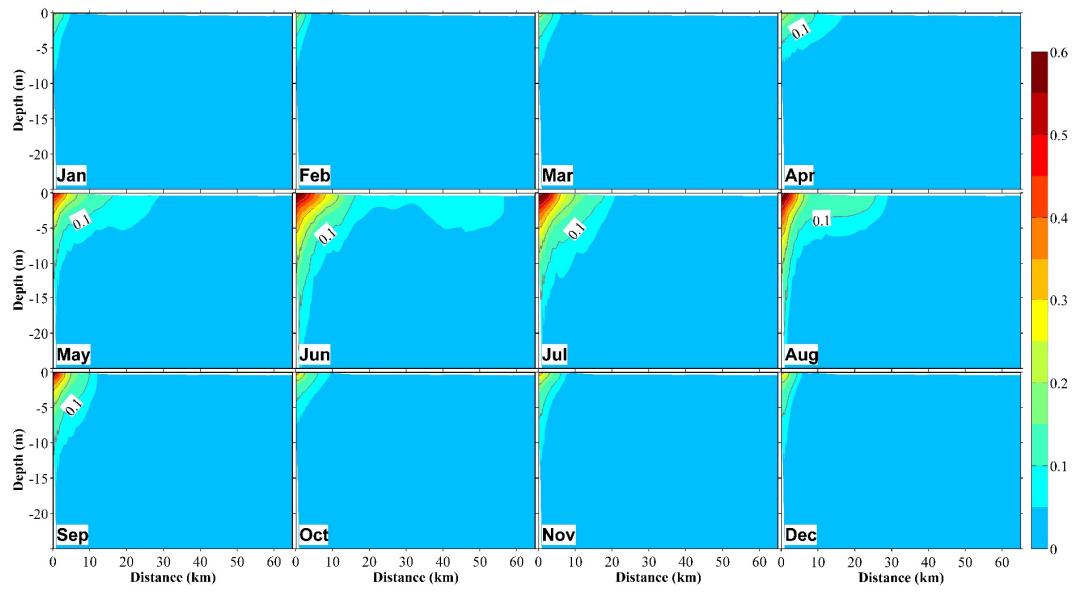


Figure S11. Vertical section (S2 in Figure 1b) of the distributions of the proportions of phytoplankton supported by nutrients originating from river water to the total phytoplankton in different months.

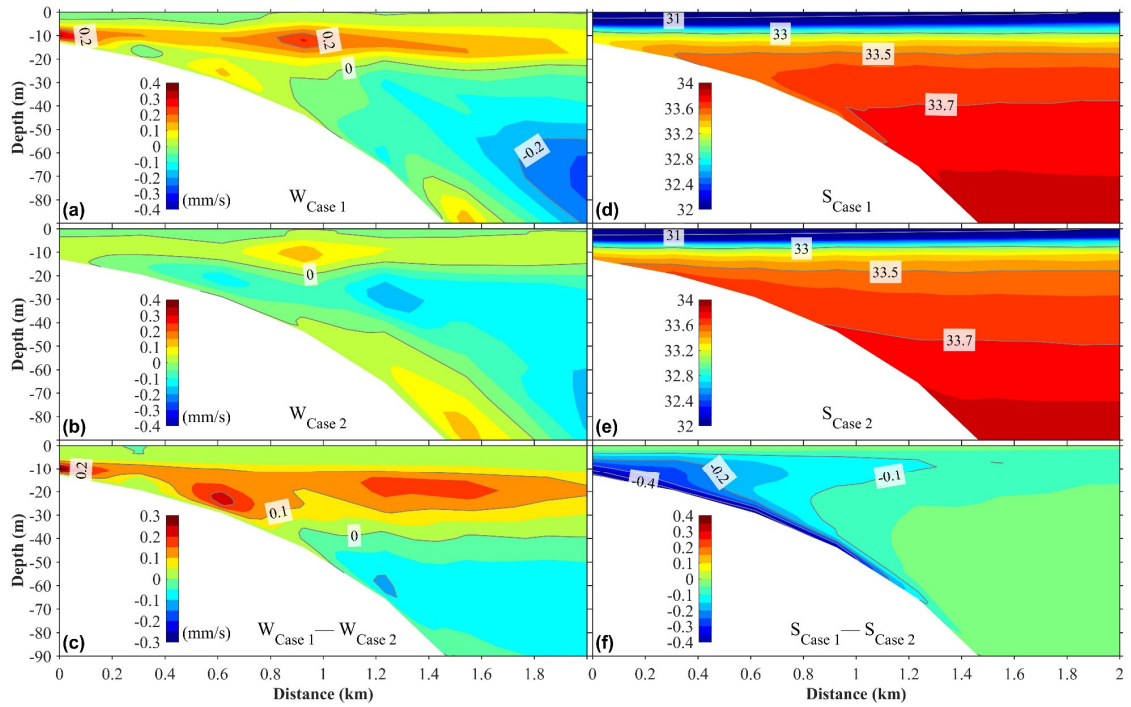


Figure S12. (a) and (b) show the vertical distributions of annual mean vertical velocity of calculations with (Case 1) and without (Case 2) buoyancy effect of SGD in the hydrodynamic model, and (c) shows the difference between them. Similarly, (d) and (e) mean the vertical distributions of annual mean salinity of calculations Case 1 and Case 2, and (f) shows the difference between them.

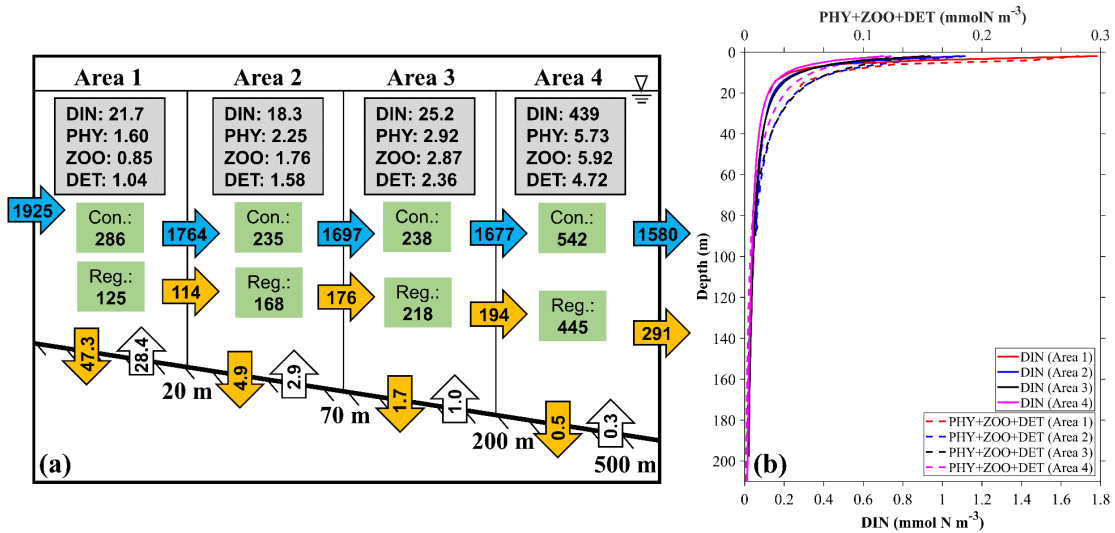


Figure S13. (a) The annual mean inventories and material flows of river-derived nutrients in 4 different areas near the outlet locations of SGD. (Area 1) 0–20 m, (Area 2) 20–70 m, (Area 3) 70–200 m, (Area 4) 200–500 m. The values in the gray rectangles represent the inventory ($\times 10^7$ mmol) of the ecosystem variables in the area. The values in the green rectangles represent the consumption (Con.) and regeneration (Reg.) rates of DIN_{RV} in the biogeochemical processes (mmol s^{-1}). The values in the vertical blue arrows represent the input transport of DIN_{RV} (mmol s^{-1}). The values in the vertical orange and white arrows represent the vertical flux to the sediment and re-decomposition flux from the sediment to the sea (mmol s^{-1}). The values in the horizontal blue and orange arrows represent the horizontal transport of DIN_{RV} and its related biological particles ($\text{PHY}_{\text{RV}}+\text{ZOO}_{\text{RV}}+\text{DET}_{\text{RV}}$) (mmol s^{-1}). (b) show the average profile of DIN_{RV} , PHY_{RV} , and DET_{RV} in these 4 areas.

References

- Blumberg, A. F., & Mellor, G. L. (1987). A description of a three dimensional coastal ocean circulation model. In N. S. Heaps (Ed.), *Three-Dimensional Coastal Ocean Models* (Vol. 4). American Geophysical Union.
- Eppley, R. W. (1972). Temperature and phytoplankton growth in the sea. *Fishery Bulletin*, 70(4), 1063–1085.
- Mellor, G. L. (1998). *USERS GUIDE for OCEAN MODEL. Program in Atmospheric and Oceanic Science*.
- Onitsuka, G., & Yanagi, T. (2005). Differences in ecosystem dynamics between the Northern and Southern parts of the Japan Sea: Analyses with two ecosystem models. *Journal of Oceanography*, 61, 415–433. <https://doi.org/10.1007/s10872-005-0051-1>
- Sarmiento, J. L., & Gruber, N. (2006). *Ocean Biogeochemical Dynamics*. Princeton: Princeton University Press. Retrieved from <https://doi.org/10.2307/j.ctt3fgxqx>